MEMORANDUM REPORT BRL-MR-3764

BRL



# PREPARATION OF HAFNIUM CARBIDE BY DYNAMIC COMPACTION OF COMBUSTION SYNTHESIZED MATERIAL

RALPH F. BENCK
LASZLO J. KECSKES
PAUL H. NETHERWOOD, Jr.



JUNE 1989



U.S. ARMY LABORATORY COMMAND

BALLISTIC RESEARCH LABORATORY
ABERDEEN PROVING GROUND, MARYLAND

TABLE OF CONTENTS



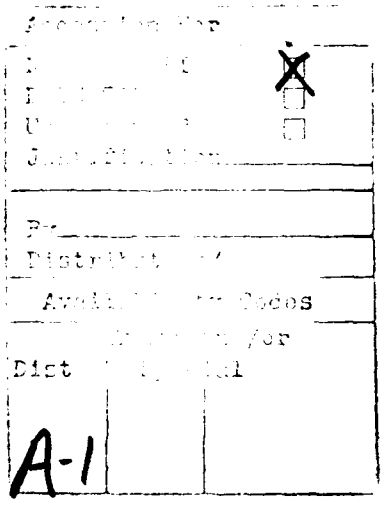


LIST OF FIGURES

ACKNOWLEDGEMENT

The measurement and analysis of the X-ray diffraction patterns of the various hafnium materials by Dr. P.W. Kingman of the BRL are gratefully acknowledged.

# 1. INTRODUCTION

Fully dense ceramic carbides possess physical properties that result in superior performance in many applications. However, the inefficient and energy intensive methods currently used for their production in most cases render them economically uncompetitive. The usual methods to produce carbides involve heating the metal oxide or the pure metal with carbon in a graphite furnace at high temperatures under an inert atmosphere. The resulting carbide powder is then sintered at high temperatures and at pressures for relatively long periods of time to produce a solid carbide. Recently, however, a more energy-efficient method of preparation has been proposed, i.e. Dynamically Compacting the Self-Propagating High-Temperature Synthesis product (DC/SHS).[1]

Of the ceramic carbides, hafnium carbide (HfC) is of interest as it is one of the most refractory materials known. HfC has a maximum melting point (which apparently occurs on the hafnium-rich side of stoichiometric composition) of 3,887 +/- 150°C.[2] Gray colored HfC, with a density of 12.7 g/cm$^3$, is the only intermediate phase found in the hafnium-carbon binary system.[3] This interstitial carbide can exist over a range of compositions, below and up to the stoichiometric composition. There are a number of reviews of the properties of HfC in the literature.[3-9] The current research is directed toward establishing the feasibility of producing solid, dense HfC by dynamically compacting the product of a SHS reaction of Hf and C powders, shortly after the SHS reaction takes place.

SHS is a highly energetic exothermic process that involves the propagation of a solid-solid combustion front through a green powder compact. Once the SHS process has been initiated, the heat of reaction is sufficient to sustain the reaction until all of the reactants have been consumed. These SHS reactions occur at temperatures in excess of 2,000°C, a temperature that is high enough to cause the evolution of most of the contaminants on the reactant powders. Although the final products have lower impurity levels than those on the precursor powders, the evolution of these impurities at the high reaction temperatures causes the formation of a highly porous reaction product. An additional source of porosity in SHS-reacted samples is that the specific volume of the green compact is greater by approximately 20 percent than that of the reacted product. As a result, the usual product of an SHS reaction can exhibit up to 50 percent porosity.

Because of the high SHS reaction temperatures, a reacted SHS product, if it is thermally insulated, can remain at a temperature that is usually above the ductile-brittle transition temperature of the material.[1] Therefore, if the SHS reaction product is consolidated at the cessation of the reaction, (while the SHS material is still hot and ductile), the porosity can be reduced to acceptable levels.

Explosive compaction was chosen as the technique to consolidate the SHS product thereby increasing its density and integrity. Explosives are finding wider use as a cheap and convenient source of high pressures for brief periods of time. Applications include welding, metal forming, and powdered material compaction. Additional examples of explosive compaction

can be found in the International Conferences on High Energy Rate Fabrication (Ref. 10) and other reference works (Refs. 11-13).

A critical element in compaction work is the design of fixtures which will achieve both complete compaction and permit the product to be recovered in useable condition. Ceramics, which require very high pressures to fuse the particles, present a particular problem in this respect, as well as being subject to fracturing from shock reverberations. Preheating the material, using either an external heat source or the heat from an SHS reaction, reduces the amount of energy needed to achieve consolidation.[14,15]

## 2. EXPERIMENTAL TECHNIQUE

2.1 Overview. When a flame source is brought near a free-standing green compact of hafnium metal and amorphous carbon powders in air, there is a very bright flash and rapid burn, followed by a slow burn and formation of a crumbly white powder. X-ray diffraction analysis indicates that this white powder is hafnium oxide ($HfO_2$). Apparently, after the completion of the SHS reaction, while the HfC is still at high temperature, the product readily oxidizes, forming CO and $HfO_2$. If the sample is semi-confined by placing the powder mixture in a suitable fixture before ignition and then smothered (e.g. with sand) within a few seconds after the initial burn, X-ray analysis shows that the product is hafnium carbide. The HfC produced in this manner is a low density, highly porous material as is illustrated in Figure 1.

The experiment design presented here was evolved in the course of a program in which SHS-produced TiC and $TiB_2$ were explosively compacted.[16] The requirements for the explosives' part of the design were that the system be safe, economical, and scaleable to large sizes. Blasting explosives with a low detonation velocity were used to minimize the shattering effects of reflected shock waves. Tests using sealed steel cases achieved satisfactory compaction with thin samples, but demonstrated that the cases could not deform sufficiently to complete the compaction of thicker specimens. The solution was to use freely moving steel plates that compressed the containment fixture. The following general procedure for the preparation of HfC was used. A mixture of hafnium and carbon powders was ball milled and pressed into a Hf-C green compact. The green compact was placed in a crushable fixture, ignited, and then, after allowing the entire sample to react, was compacted by explosively propelling a flat steel plate onto the hot sample. Table 1 lists the experiments that were performed.

The initial experiments, (tests 1-3) shown in Table 1, were designed to determine whether the SHS reaction would propagate through an Hf-C green compact fixtured for compaction. Tests with modified fixtures intended to better confine the reacting compact (tests 4-6, 8-11) were then performed. Experiments to increase the heat available to the HfC-SHS reaction were undertaken in tests 7, 12, and 14.

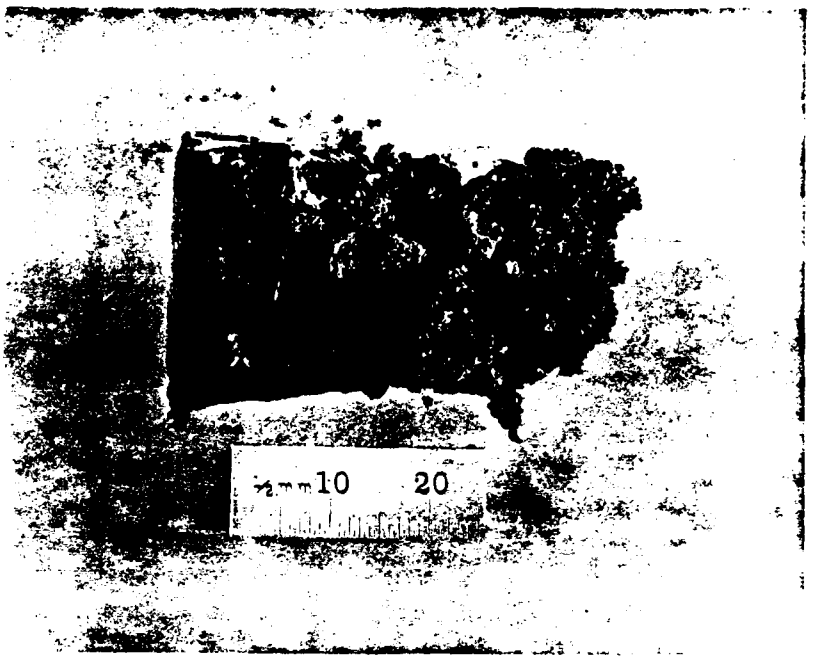


Figure 1. Uncompacted HfC, initially 25.4 mm thick.

In these tests another SHS system, either Ti-C or Ti-B, was added to the HF-C system so that the excess heat given off by the second SHS reaction would promote the formation of HfC (i.e. "chemical furnace"). In test 7 approximately 50 g of a Ti-C mix was placed on the top of the Hf-C green compact, while in test 12 the Hf-C green compact was surrounded with approximately 400 g of a Ti-C mixture. In test 14 the Hf-C green compact was surrounded with approximately 400 g of a Ti-B mixture. Two experiments were also conducted to determine if an internal source of heat would be beneficial by mixing Ti with the Hf and C and forming a mixed carbide. The procedures for the mixed carbides were identical to those with Hf alone, except that the initial mixture included Ti metal powder as well as Hf and C (tests 13 and 15).

TABLE 1. HfC Feasibility Studies.

| Test # | (A) Sample dia. [mm] | (B) Fixture (1) [mm] | (C) Plate thick. [mm] | (D) Explosive thick. [mm] | (E) Barrier (2) | Density final(3) [g/cm$^3$] |
|---|---|---|---|---|---|---|
| 1 | 31.8 | 31.8 | 12.7 | 19.0 | none | 10.5 |
| 2 | 31.8 | 31.8 | 25.4 | 19.0 | none | 10.7 |
| 3 | 50.8 | 50.8 | 25.4 | 25.4 | none | 11.3 |
| 4 | 50.8 | 57.2 | 25.4 | 25.4 | Grafoil | 11.5 |
| 5 | 50.8 | 57.2 | 25.4 | 38.1 | Grafoil | 11.1 |
| 6 | 50.8 | 57.2 | 25.4 | 25.4 | gap | 9.7 |
| 7 | 31.8 | 57.2S | 25.4 | 25.4 | Ti-C | 9.1 |
| 8 | 31.8 | 50.8 | 25.4 | 25.4 | brick | 9.4 |
| 9 | 31.8 | 50.8 | 25.4 | 25.4 | Grafoil | 9.1 |
| 10 | 31.8 | 57.2S | 12.7 | 19.0 | comb. | 9.4 |
| 11 | 31.8 | 50.8 | 6.4 | 12.7 | comb. | 8.9 |
| 12 | 31.8 | 101.0 | 25.4 | 38.1 | Ti-C | 11.0 |
| 13(4) | 50.8 | 101.0 | 25.4 | 25.4 | brick | 7.1 |
| 14 | 50.8 | 101.0 | 25.4 | 25.4 | Ti-B | 10.9 |
| 15(5) | 50.8 | 101.0 | 19.0 | 38.1 | brick | 9.7 |

NOTES:
Columns (A)-(E) correspond to the similarly designated structures illustrated in Figure 2.

(1) Dimensions are for inner diameter of the round or the inner lengtn of a side of the square, S, fixtures.
(2) Material placed between green compact and fixture.
(3) Measured by water displacement technique.
(4) Green compact made from a mixture of Hf and Ti(1:1) with C.
(5) Green compact made from a mixture of Hf and Ti(3:1) with C.

2.2 Experimental Procedure. The experiments listed in Table 1 are variations of a basic procedure for producing titanium carbide and titanium diboride. A schematic diagram with the pertinent experimental details keyed to Table 1 is shown in Figure 2. Detailed discussions of the individual steps in the procedure are provided below.

Aliquots of Hf metal and amorphous C powders were weighed out and mixed for 30 minutes in a ball mill. A description of the powders is presented in Table 2. The stoichiometry of the initial reactants was varied from a Hf:C mole ratio of 1:1 to 1:0.8. The phase diagram of Hf-C[4,17] indicates that the temperature needed to melt the SHS product and to produce a liquid phase is lower where there is an excess of Hf so the majority of the tests were made with the 1:0.8 mixture. This mixture was formed into a green compact by uniaxially pressing at pressures in the range of 27 to 69 MPa in either a 31.8- or 50.8-mm diameter cylindrical steel die. The height of the green compact was approximately 25 mm.

TABLE 2. Description of Powders.

| Designation | Size [μm] | Purity [%] | Description | Manufacturer |
|---|---|---|---|---|
| AE Hf | -44 | 99.+ | Hafnium | Teledyne Wah Chang* |
| AE Ti | -44 | 99.7 | Titanium | Atlantic* |
| STR C | 0.05 | 99.5 | Sterling R carbon 99.5% fixed C content | Cabot** |

*Atlantic Equipment Engineers, Bergenfield, NJ.
**Cabot Corporation, Boston, MA.

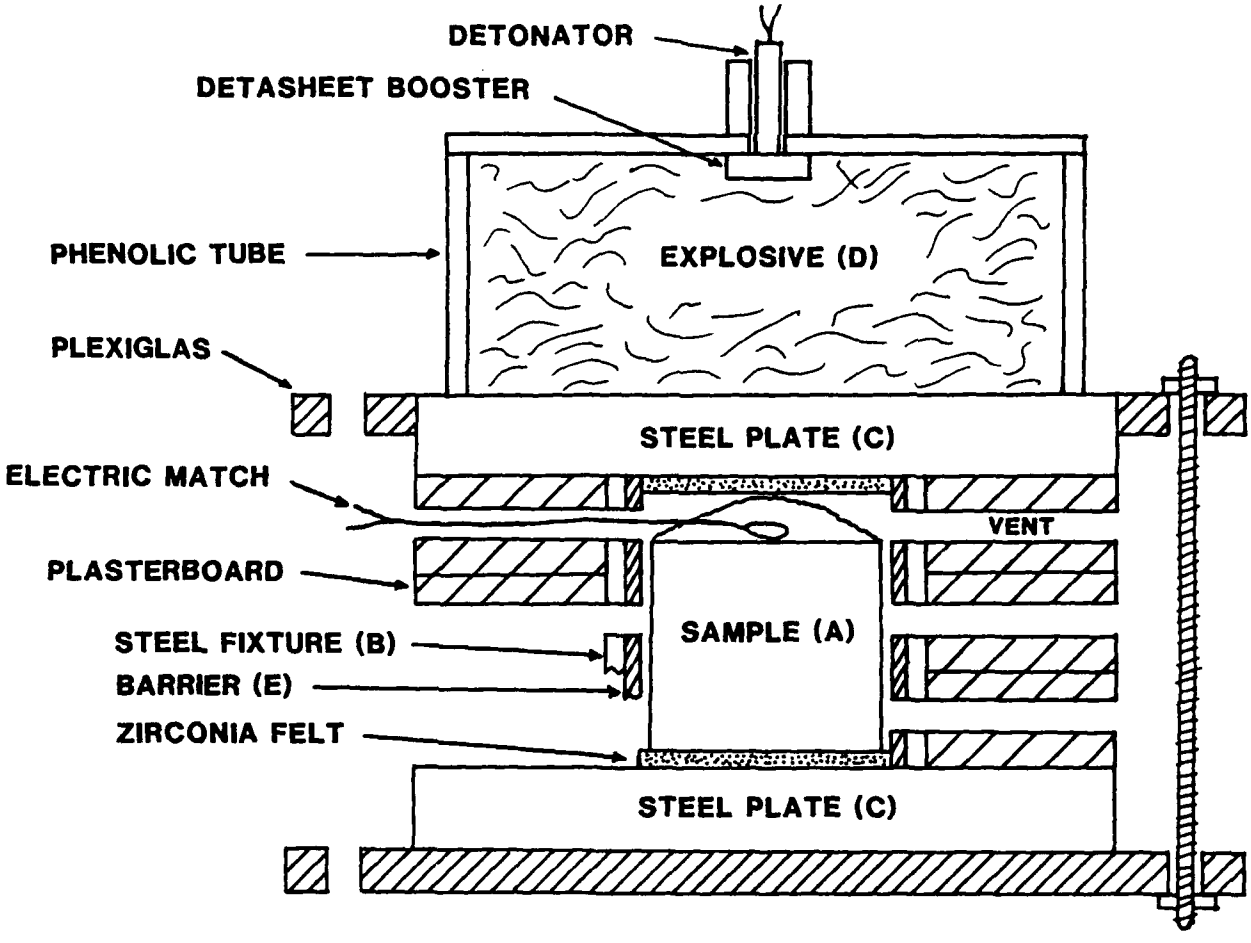


Figure 2. Schematic diagram of experimental setup. Structures (A)-(E) correspond to data presented in Table 1.

The green compact was inserted into a 1.6-mm thick, 38.1-mm tall, steel containment fixture. Usually, the fixture was a section of a round, mild steel pipe, but in two experiments a section of square pipe was used. Copious quantities of gas are released during the SHS burn phase of the procedure. Gas escape paths were provided by drilling three rows of four one-quarter inch holes equally spaced around the circumference at the top, midline, and bottom of the fixture. The sides of the pipe assembly were surrounded with three layers of 12.7-mm thick gypsum drywall (plasterboard/sheetrock). The gypsum drywall functioned as an insulator and a crushable medium needed for uniform compaction. The area of the gypsum drywall was kept the same as the area of the top and bottom steel plates. Vent holes, opposite the holes in the retaining fixture, were bored through the width of the gypsum drywall so that there was a clear path for escaping gases.

An electric match was placed on the top of the compact, with the leads of the match brought out through one of the gas escape holes in the retaining fixture. A small amount (10-15 g) of a 1:2 mole ratio mixture of Ti and B powders (the igniting mixture) was placed on the top of the Hf-C compact and lightly pressed into place around the electric match. This igniting mixture was necessary because direct ignition by an electric match of the Hf-C powder compact was not consistently successful.

A piece of 1.3- or 2.5-mm thick zirconia felt, the same diameter as the containment fixture, was placed between the top of the sample and the top steel plate (Zirconia Felt, Zircar Products, Inc., 110 North Main Street, Florida, New York. ZYF-50, 1.3-mm thick; ZYF-100, 2.5-mm thick; 96 percent porosity). A

similar piece of felt was placed between the bottom steel plate and the bottom of the sample. The felt served as an insulator to thermally isolate the sample. The steel containment fixture-gypsum drywall package was placed between two 15.2-cm square steel plates. Various thicknesses and kinds of steel (Mild Steel, RHA, High Hard) were used. The heat from the SHS reaction can release enough gas to push off an unsecured top plate. To keep the top and bottom plates in register and to give a measure of protection to the explosives on the top plate from the usually violent SHS reaction, the edges of the bottom and top plates were encased in a 6.4-mm thick sheet of polymethyl methacrylate (PMMA) and bolted together with four 6-32 threaded brass rods. There was no PMMA between the sample and the steel plates.

A 15.2-cm diameter phenolic tube was centered and epoxied to the upper surface of the top steel plate and filled with DBA-10HV explosive (DBA-10HV Slurry Explosive, Ireco Chemicals, 3000 West 8600 South, West Jordan, Utah). The thickness of the explosive charge, as shown in Table 1, was varied from 12.7 to 38.1 mm. A 2 x 2 x 0.6-cm thick piece of Detasheet C, centered on the underside of a 3-mm thick PMMA cover plate, was used as a booster. A J-2 detonator initiated the booster explosive. This design has the advantage of allowing modular construction so that the explosive driver package can be assembled separately from the SHS combustion package and the two units combined just prior to firing. The explosive driver system was originally designed to load large samples using sweeping detonation waves. Since the HfC specimens were no larger than 50 mm in diameter, the experiments were simplified by the use of centrally initiated charges.

The assembly was partially buried on the top of an approximately 2-m tall sand pile with the lowest gas vent just above the surface of the sand. The electric match was remotely activated, igniting the starting powder that, in turn, ignited the Hf-C green compact. The explosives were detonated approximately 8 s after the SHS reaction was initiated. Earlier experiments indicated that it should have taken approximately 5 s for the Hf-C compact to completely react. The detonation drove the hot HfC pellet and steel plates several inches into the sand pile, covering the whole assembly with sand. The sample was allowed to cool for at least 30 min in the sand before recovery.

It should be noted that the combination of SHS with explosive compaction requires care in design and execution. The SHS reactions are generally violent, producing jets of flame and hot particles, and the gases evolved can force components of the experiment apart. The explosive charge must be protected from the heat and flames of the SHS reaction, but elaborate measures are not required. The steel plate used here is an effective barrier during the reaction time. Vent holes direct the flames away from the explosives so that plastic parts of the experiment can survive the brief interval between sample ignition and explosives detonation. As specimen size increases, the design must be modified to cope with larger forces and longer times.

## 3. RESULTS AND DISCUSSION

The final products of tests 1-3 were cracked and friable because there was no barrier placed between the retaining ring

and the green compact as is indicated in Table 1. These specimens were attracted by a magnet, indicating that they were grossly contaminated with iron. In tests 4-6 there was no gross iron contamination but the ceramics were cracked. X-ray analysis indicated that the material formed was HfC, but Scanning Electron Microscopy (SEM) showed that there was very little interparticle bonding. The ceramic disks produced in the remainder of the experiments were basically sound, although they contained some cracks and were not fully dense. Several parameters have been identified as being important in the preparation of HfC. These are sample containment, contamination, total heat available to the reaction, explosive loading, and precursor powder characteristics. Each of these factors will be discussed in more detail below.

3.1 Preparation Parameters. The containment fixture must restrain lateral motion of the reacted material while allowing vertical compaction. Lateral motion of sample material results in lower density and shear cracking of the specimen edges. The vertical motion is large, as the final thickness of the specimen is approximately one-third of the initial height of the assembly. Low porosity, rigid materials will not compact enough to allow this vertical motion, while high porosity material will either not survive the SHS burn phase or will not provide sufficient edge support. Lateral support was provided by a thin (1.6-mm wall thickness) steel ring. The steel ring must survive the reaction and retain enough strength to contain the sample, but must be weak enough to collapse readily in the direction of compaction. Ring deformation can be improved by arranging the vent holes to cause the ring to buckle symmetrically during compaction.

The ring can be a source of iron contamination if it melts during the SHS reaction or after compaction. To prevent this contamination, either an air gap or some other type of barrier was placed between the inside of the ring and the green compact. The various barriers that were used are listed in Table 1. In Table 1 "brick" refers to portions of 1,500°F MgO insulation firebrick, and "comb." is a solid section of firebrick placed between the containment fixture and the sample with the sample surrounded by Grafoil (Grafoil, flexible graphite sheet, 0.4 mm thick. Union Carbide Corp., Electronics Division, Specialty Products Group, Cleveland, OH.). While the use of an air gap reduced the iron contamination, the gap caused the edges of the sample to be excessively fractured. Thin Grafoil sheets or thick firebrick insert barriers eliminated the gross iron contamination. The samples produced with the firebrick were fractured more than those that were only surrounded with Grafoil.

In tests 7, 12, and 14, green compacts of either Ti-C or Ti-B mixtures were placed around the Hf-C green compact to provide extra heat. The number of moles in the Ti-C or Ti-B green compact was approximately 10 times the number of moles in the Hf-C green compact. The primary function of the "chemical furnace" was to preheat the Hf-C green compact before the onset of the HfC SHS reaction. Such external heating acts to elevate the compact temperature and stabilize an otherwise unstable or weak exothermic reaction. Another function of the chemical furnace was to provide the shock-consolidated HfC with external heat during post-sintering. The ceramic formed in these three experiments was of good integrity but graded, ranging from what

appeared to be TiC or $TiB_2$ to HfC. The densities shown for these tests in Table 1 are for samples taken only from the apparent HfC portion. The degree of mixing the two ceramics with each other was not determined. The HfC produced in these three tests was less cracked and more dense than equivalent samples produced without the added Ti-C or Ti-B.

Efforts to produce mixed Hf-Ti carbides (tests 13 and 15) were successful, as both of the mixtures ignited and burned well during the SHS phase of the procedure, and the final compacts were relatively hard and free of cracks. The measured density of the 1:1 mixture was 83 percent of theoretical density (% T.D.), while the 3:1 sample was 93 % T.D., assuming that the method of mixtures is applicable in determining density for these systems. The function of titanium in the Hf-C green compact is twofold. First, unlike the experiments with external heat sources, the heat from the synthesis of titanium and carbon in the powder mixture is generated internally. As a result, any heat emanating from the TiC reaction and TiC product is in direct contact with the Hf and C powders and would increase the total heat available for the Hf-C reaction or sintering. Second, TiC is more resistant to oxidation than is HfC at elevated temperatures. Kinetic oxidation curves above 1,000°C reveal that HfC oxidizes at a rate that is approximately seven times faster than that of TiC.[18] Therefore, while the addition of TiC may not eliminate post-reaction oxidation of HfC, it may act to stabilize HfC and improve its resistance to such oxidation.

Compaction is a function of plate hardness, plate thickness, and explosive loading. The HfC disks, formed using RHA (Brinell Hardness Number [HBN] 300-400) or High Hard steel (HBN 477-534)

plates, had flat top and bottom surfaces and were relatively crack free. The mild steel (HBN 150-250) plates deformed under loading and the HfC disks formed with their use had domed top and bottom surfaces and generally contained networks of horizontal cracks. The best appearing compaction was produced by using 25.4 mm of explosive on a 25.4-mm thick plate; however, this was not sufficient to achieve complete consolidation of the ceramic.

The morphologies of the reactant powders used in this investigation were examined with SEM. A brief description of the starting powders is presented in Table 2. Photomicrographs of the precursor powders are shown in Figure 3 with STR C in 3a, AE Hf in 3b, and AE Ti in 3c. The STR C has very small but uniform particles of approximately 0.05 μm which tend to agglomerate into larger, 10-20 μm rounded particulates. The hafnium powder consists of particles that are somewhat larger than the carbon particulates, and the distribution in their sizes and shapes is also broader. The Hf particles are approximately 40 μm, irregularly shaped fragments, with sharp edges and cleavage facets. The titanium particles are irregular, with relatively smooth surfaces, some with rounded and some with sharp edges. Individual particles are generally elongated with dimensions of approximately 20-40 μm.

An SHS reaction will be local, uneven, and nonuniform if it cannot develop a uniformly propagating reaction front.[19] It is, therefore, essential that the precursor powders be uniformly mixed. The hafnium and carbon powders described above behave non-ideally during mixing. A major reason is that high purity amorphous carbon agglomerates via electrostatic attraction between submicron particulates. It is speculated that during

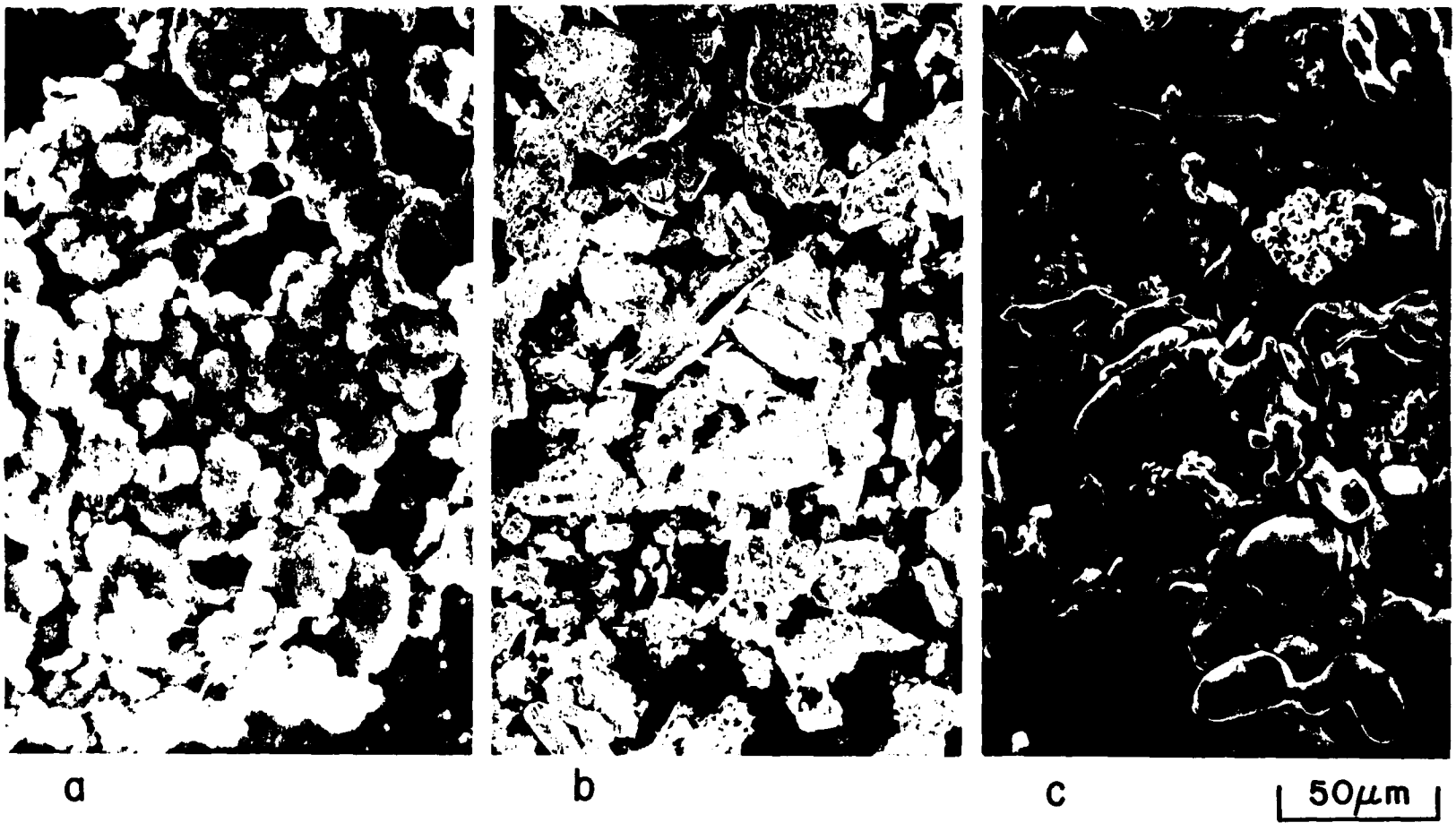


Figure 3. Scanning Electron Micrographs of the starting powders. The STR C powder is shown in 3a, AE Hf powder in 3b and AE Ti in 3c. Magnification of 500x in all micrographs.

mixing, without flow agents to aid deagglomeration, the agglomerates will not be uniformly dispersed, and, consequently, the carbon will not be evenly distributed. Additional segregation in the mixture can arise from differences in settling rates during mixing between the carbon agglomerates and the much denser hafnium particles. As a result of incomplete mixing, the shock-consolidated sample will consist of partly reacted HfC grains intermixed with unreacted excess hafnium particles and carbon agglomerates. Evidence of incomplete mixing is shown in Figure 4 where an interior surface of sample 8 exhibits thin, almost lenticular masses of unreacted carbon interspersed within the HfC body. In the figure, the dark rounded areas are the unreacted carbon and the lighter areas are HfC.

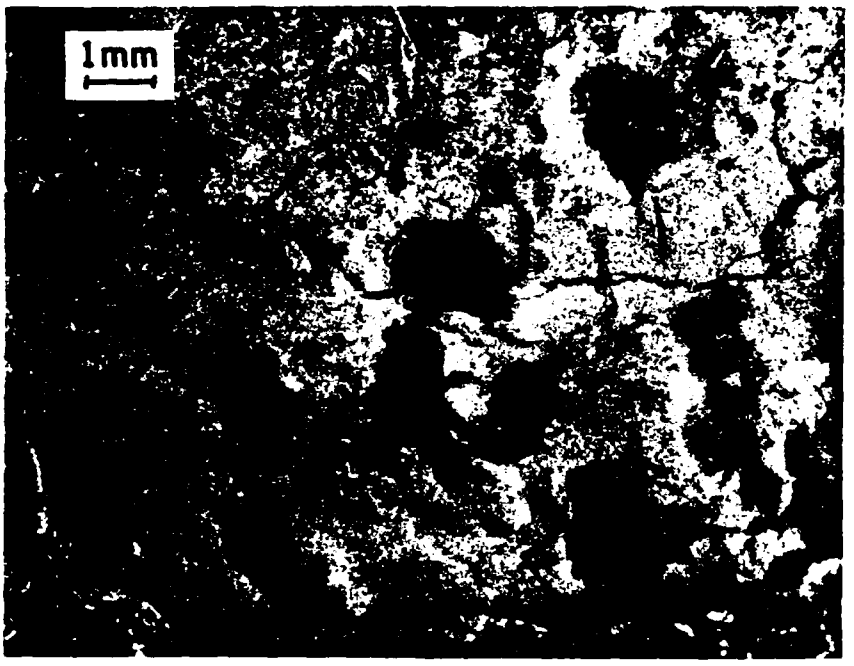


Figure 4. Photomicrograph of an interior surface of sample 8.

3.2 Sample Microstructure and Reaction Characteristics.

SEM examination of the reaction products revealed that the interior microstructure of all the reacted HfC bodies consisted of HfC grains fused into bands, individual or partially sintered HfC grains, and voids. Most of the HfC samples showed interconnected bands that were interspersed with open porosity. Figure 5 shows a diamond polished surface of a HfC sample where the light areas are void-free hafnium carbide and the darker areas are open pores. As can be seen in the figure, the average band size is approximately 50 μm and the average pore size is approximately 10 μm. Pore edges appear highly angular, and although there is evidence of some sintering in the sample, the intergrain bonding appears to be weak.

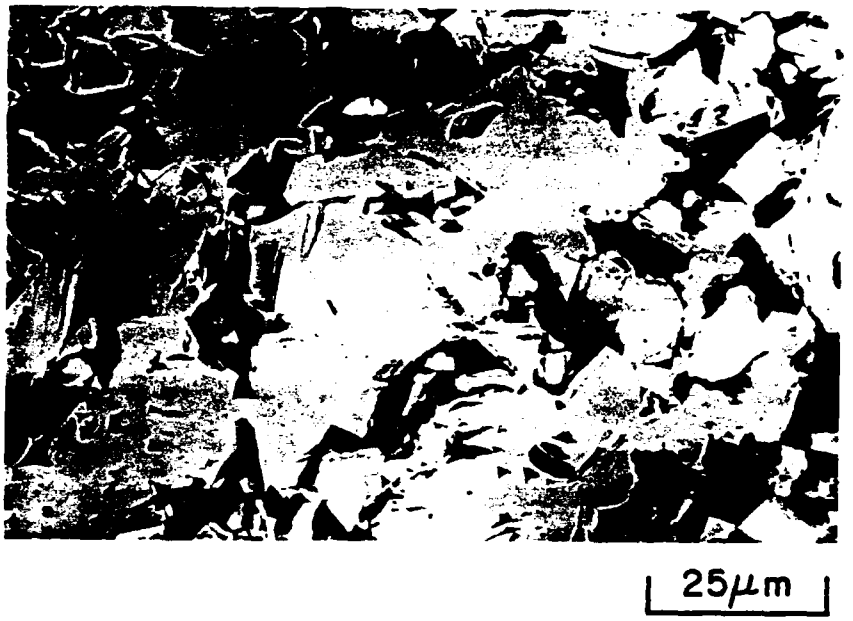


Figure 5. Polished surface of sample 5. Magnification of 1,000x.

The poor bonding and lack of extensive sintering of the HfC samples can be explained by considering the characteristics of the SHS process. In an SHS system, heat that is generated in the reaction zone is dissipated via conduction and radiation. For self-propagation to occur, the dissipated heat must raise the unreacted compact close to its ignition temperature.[19] Similarly, for good post-reaction bonding, sufficient heat must be available to sinter the product. If the heat of formation is small, i.e. the system is only weakly exothermic, the reaction may quench and not propagate. The heat of formation of HfC is quite high, -50 kcal,[20] but in the configuration used in the present study, this heat may not have been enough to provide both preheating and post-reaction sintering. This is probably due to the high melting temperatures of both hafnium (M.P. 2,150°C) and the HfC product (M.P. 3,887°C). Since X-ray diffraction analysis studies showed that HfC was formed, it can be concluded that preheating occurred and the reaction propagated. However, since the samples exhibited poor interparticle bonding, there probably was insufficient heat for complete post-reaction sintering.

The microstructures of the mixed Hf-Ti carbides were different from those where only HfC was present. The porosity of the mixed carbide samples increased with increasing amounts of titanium. While the porosity in the mixed carbides is pronounced, unlike the HfC, they show extensive melting of grains. The molten appearance implies that there must have been more heat available during the post-reaction phase than in those with only Hf present. The consequences of such melting may be that a better interparticle bonding exists among grains. Figure 6 shows the polished surfaces of three samples where the ratio of

titanium to hafnium is increased. In Figure 6a (sample 10 with only hafnium present), the polished surface shows better interparticle sintering than shown in Figure 5, but the pore morphology remains similar. The pore edges are distinct and sharp. The improved sintering in sample 10 is most likely attributed to better thermal insulation; see Table 1. As the amount of titanium is increased, the effects of melting are more pronounced. In Figure 6b with a Hf to Ti mole ratio of 3:1 there is evidence of rounding in pores, and some grains show interparticle necking. A close observation of pore interiors reveals that melting does not occur throughout the sample. As seen in Figure 6c, when the Hf to Ti mole ratio is 1:1, practically all pores are rounded, and the pore walls show extensive interparticle necking and melting of some grains.

Clearly, increasing the amount of TiC enhances the interparticle sintering and bonding in the product. However, the role of TiC in the TiC-HfC system is complicated because the two carbides form a solid solution without a distinct separation of TiC and HfC grains, i.e. a eutectic duplex structure. References 17, 21, and 22 report that the solid solution is not continuous below 1,900°C, but limited, with a miscibility gap between 28 and 94 mol. percent of TiC in HfC. The effect of this gap is that instead of a single continuous phase, $\alpha$, forming between the two carbides, two intermediate phases, $\alpha_1$ and $\alpha_2$, will form. Without the use of X-ray diffraction or differential thermal analysis, the phase separation and the ratio of $\alpha_1$ to $\alpha_2$ in the shock-compacted samples could not be confirmed.

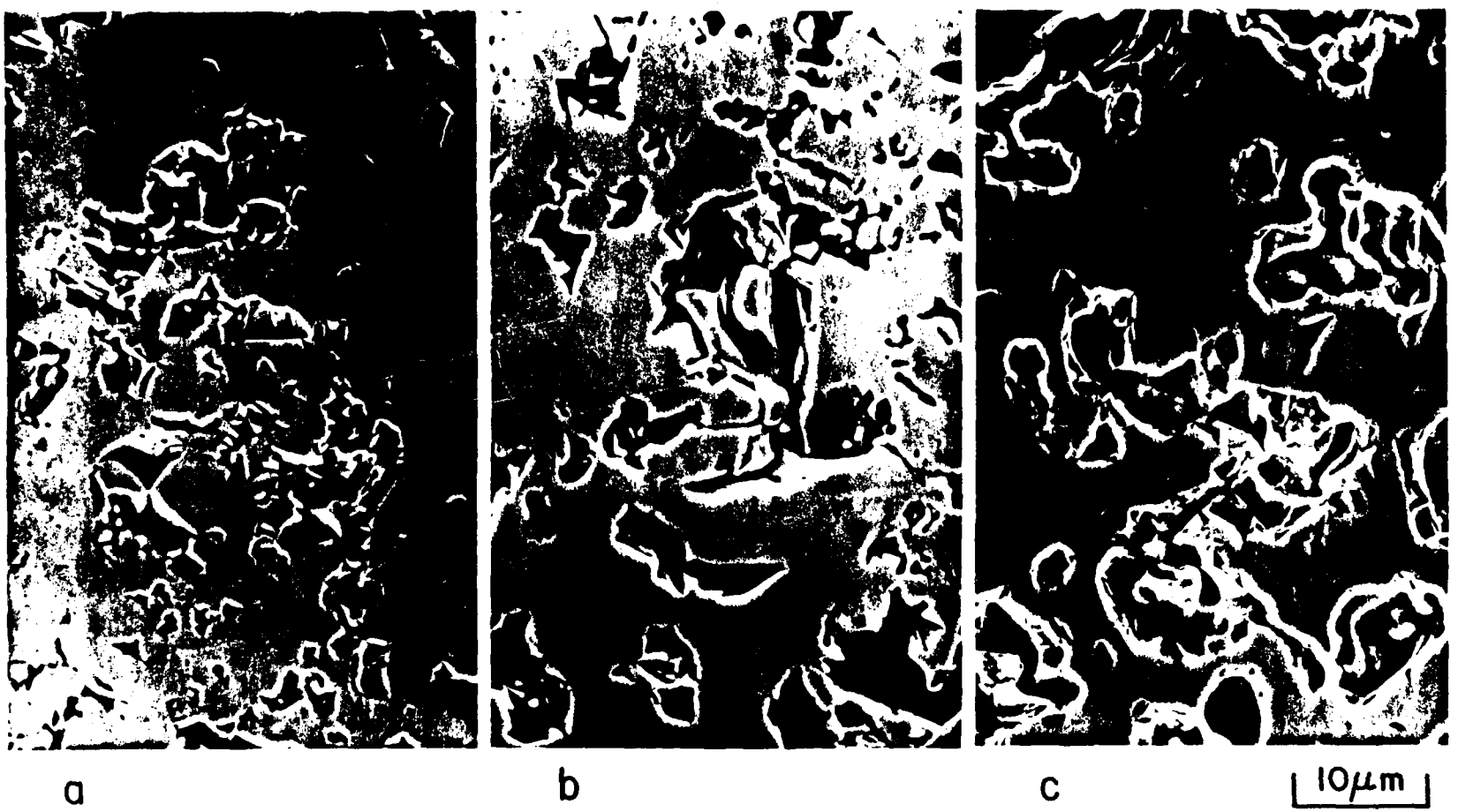


Figure 6. Polished surfaces of HfC samples with sample 10 (Hf only) shown in 6a, sample 15 (3:1 Hf:Ti) in 6b, and sample 13 (1:1 Hf:Ti) in 6c. Magnification of 2,000x in all micrographs.

3.3 Fracture Characteristics. At room temperature, the HfC samples generally failed via transgranular and intergranular brittle fracture. As seen in Figure 7, the fractographs of sample 10 reveal that the mode of failure depends on the location of the fracture region in the sample. The fractograph of an area close to the edge of sample 10 is shown in Figure 7a. Here, fracture occurred by intergranular separation. The facets of the grains reveal interparticle necking and bonding as well as partial melting of grain surfaces. However, such surfaces are very weakly bound. In contrast, an area closer to the center of the sample, as illustrated in Figure 7b, reveals that some grains failed by transgranular cleavage across the HfC grains with cleavage steps appearing in several grains. It may be emphasized that the grains that failed by cleavage are much larger than those that failed by intergranular fracture. Thus, where sintering effects were more dominant, i.e. sufficient heat was generated and retained longer, the material had time to develop the interparticle bonds; however, large-grain structure may not produce desirable mechanical properties.

The fracture characteristics of Hf-Ti carbides have also been examined. In Figure 8a the fractograph of sample 15 with a Hf:Ti mole ratio of 3:1 is shown. Although fracture occurs via cleavage, the interparticle bonding is relatively weak. Individual grains are readily distinguished, and interior pores show little sintering. When the amount of titanium is increased to a mole ratio of 1:1, the characteristic failure mode of the material is purely transgranular. As seen in Figure 8b, while the sample porosity is still pronounced, both the effects of extensive sintering and of strong interparticle bonding become evident. It may be noted that since the TiC-HfC system does not

form a duplex structure with easy assignments of matrix and inclusion, the overall physical properties of the product cannot be attributed to either component.

3.4 Microhardness. Knoop microhardness measurements were made on four of the Hfc samples and are presented in Table 3. Using a 100-g test load, the size of the indent produced by the diamond indentor was comparable to the HfC grain size. However, for samples that have a high degree of porosity, the individual grain hardness does not necessarily represent the overall hardness. Therefore, in order to evaluate the average overall sample hardness, a 400-g test load was also used. The indent produced with this test-load extended over several HfC grains. Although the individual grain hardnesses of the samples tested were approximately HK(100 g) 1800, the corresponding hardness values with the 400-g load were much lower, HK(400 g) 1100. As a result of the severe porosity and the substoichiometry of the samples, the hardness values are much lower than the hardness of HfC produced by other techniques.[8] The hardness values of the two Hf-Ti carbides that were produced are also included in Table 3. The addition of titanium to the HfC samples did not increase their hardness over that of HfC alone. Furthermore, both of the TiC-HfC samples were porous and it was difficult to make an accurate assessment of these HK(400-g) hardnesses.

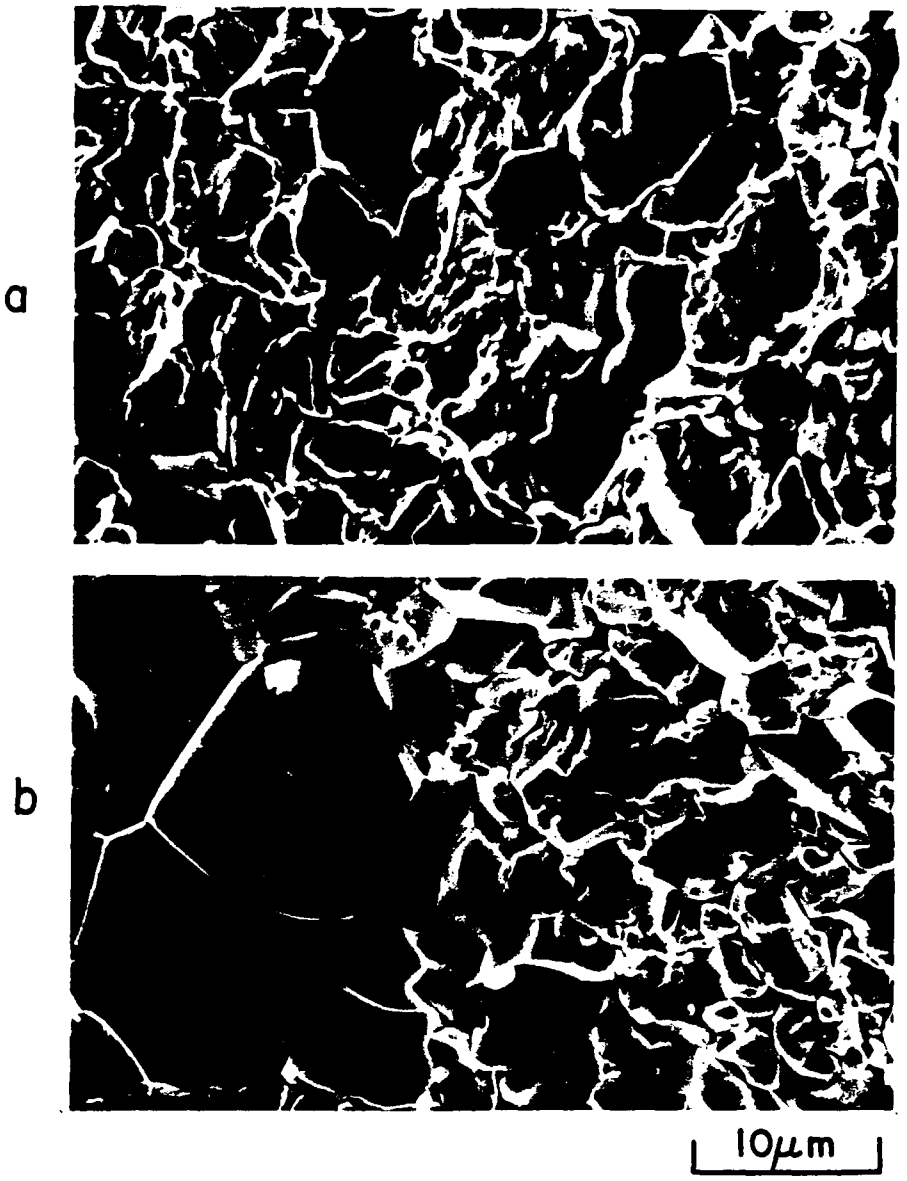


Figure 7. Fractographs of sample 10. Photograph 7a shows an area near the edge of the sample and 7b shows an area at the center of the sample. Magnification of 2,500x in both micrographs.

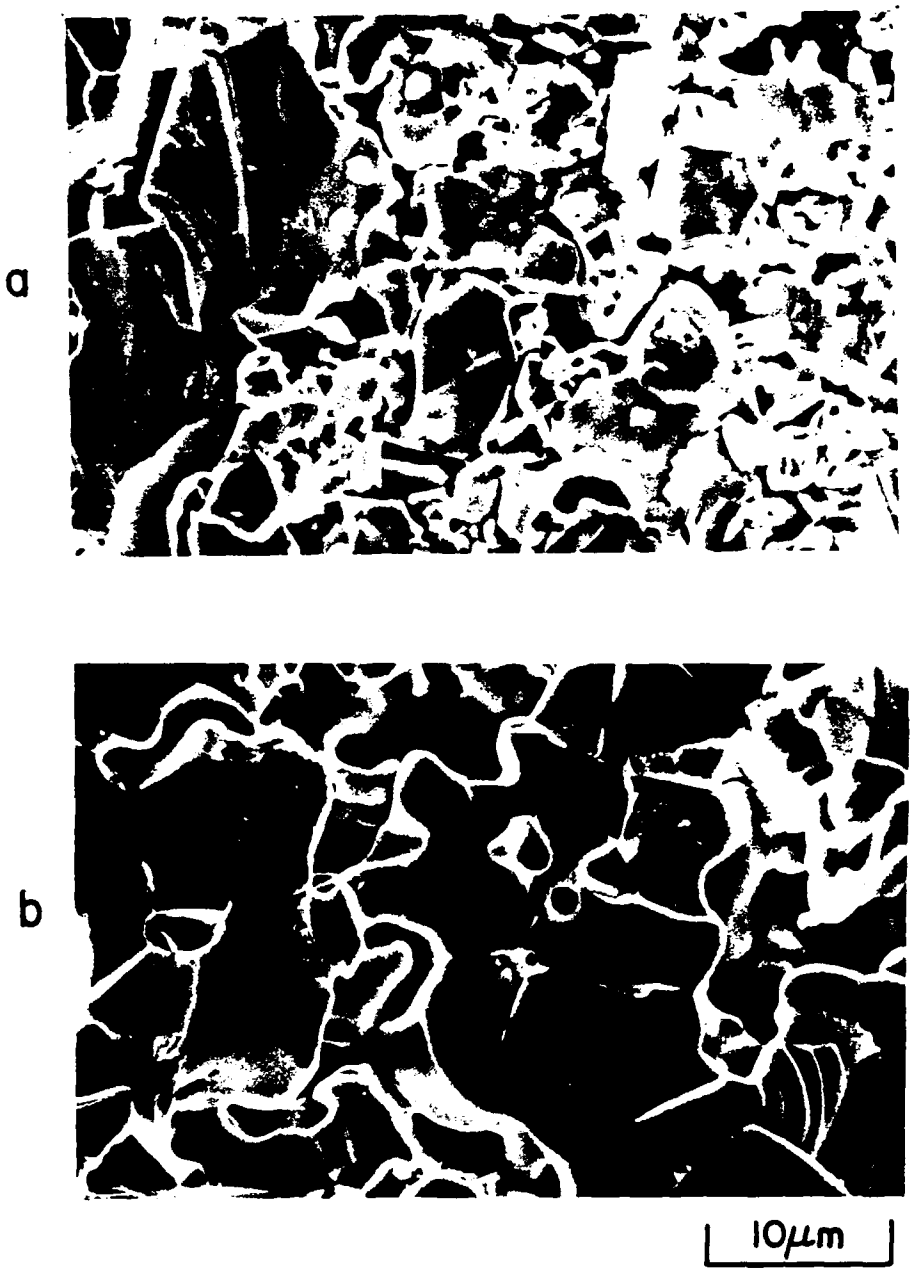


Figure 8. Fractographs of HfC samples with sample 15 (3:1 Hf:Ti) shown in 8a and sample 13 (1:1 Hf:Ti) in 8b. Magnification of 2,500x in both micrographs.

Table 3. Knoop Microhardness.

| Sample | HK (100g) [kg/mm$^2$] | HK (400g) [kg/mm$^2$] |
|---|---|---|
| Hf | | |
| 5 | 1,800 ± 400 | 1,010 ± 430 |
| 6 | 1,990 ± 180 | 1,250 ± 290 |
| 10 | 1,880 ± 410 | 990 ± 310 |
| 12 | 1,750 ± 260 | 1,280 ± 160 |
| Hf/Ti | | |
| 13 | 1,850 ± 190 | (780 ± 270) |
| 15 | 1,680 ± 290 | (970 ± 290) |

## 4. CONCLUSIONS

This study has demonstrated that solid, dense hafnium carbide can be produced by dynamic compaction of SHS-produced material. The samples, however, exhibit poor interparticle bonding and some cracking. It is concluded that the amount of heat given off by the SHS reaction is not sufficient to both propagate the synthesis reaction and properly sinter the SHS product. The procedure to prepare HfC can be improved by surrounding the Hf-C green compact with an external heat source, e.g. an SHS chemical furnace, adding additional thermal insulation, and possibly using a finer hafnium powder. Optimization of the explosive loading system could reduce cracking of the samples and improve the final density.

## 5. LIST OF REFERENCES


1. Niiler, A., Moss, G. L., and Eichelberger, R. J., Ceramics Fabrication by Shock Compaction of SHS Produced Materials, Patent Application in Progress, Ballistic Research Laboratory, Aberdeen Proving Ground, MD.

2. Agte, C. and Alterthum, H., "Systems of High-Melting Carbides," Z. Tech. Phys., Vol. 11, pp. 182-191, 1930.

3. Cotter, P. G. and Kohn, J. A., "Industrial Diamond Substitutes(I) Physical and X-Ray Studies of Hafnium Carbide," J. Amer. Ceram. Soc., Vol. 37, No. 9, pp. 415-420, September 1954.

4. Sara, R. V., "The Hafnium Carbon System," Trans. Met. Soc. AIME, Vol. 233, No. 9, pp. 1683-1691, September 1965.

5. Storms, E. K., Critical Review of Refractories I., LAMS-2674(Pt1), Los Alamos National Laboratory, Los Alamos, NM., March 1962.

6. Storms, E. K., Review of Refractories II, LAMS-2674(Pt2), Los Alamos National Laboratory, Los Alamos, NM., October 1962.

7. Toth, L. E., Transition Metal Carbides and Nitrides, New York, NY., 1967.

8. Storms, E. K., The Refractory Carbides, Academic Press, New York, NY., 1967.

9. Perry, A. J., "The Refractories HfC and HfN - A Survey, I Basic Properties," Powder Met. Int., Vol. 19, No. 1, pp. 29-38, January 1987.

10. Berman, I. and Schroeder, J. W.(Ed), The 8th Int. Conf. on High Energy Rate Fabrication, pp. 109-145, San Antonio, TX., 1984.

11. Blazynski, T. Z.,(Ed), Explosive Welding, Forming and Compaction, Applied Science Publishers, London, England, 1983.

12. Meyers, M. A. and Murr, L. E.(Ed), Shockwaves and High Strain-Rate Phenomena in Metals, Plenum Press, New York, NY., 1981.

13. Linse, V. D., Innovations in Materials Processing, Bruggeman, G. and Weiss, V. Eds., pp. 381-404, Plenum Pub. Corp., New York, NY., 1985.

14. Linse, V. D., Dynamic Compaction of Ceramics and Metals, presented at the H. J. Kraner Award Symposium: Lehigh Valley Section of the American Ceramic Society, Bethlehem, PA., 1980.

15. Gorobtsov, V. G. and Roman, O. V., "Hot Explosive Pressing of Powders," International J. Powder Metallurgy and Powder Technology, Vol. 11, No. 1, pp. 55-60, January 1975.

16. Niiler, A., Kecskes, L.J., Kottke, T., Netherwood, P.H. Jr., and Benck, R.F., Explosive Consolidation of Combustion Synthesized Ceramics: TiC and $TiB_2$, BRL-TR-2951, Ballistic Research Laboratory, Aberdeen Proving Ground, MD, December 1988.

17. Perry, A. J., "The Refractories HfC and HfN - A Survey, II Phase Relationships," Powder Met. Int., Vol. 19, No. 2, pp. 32-36, February 1987.

18. Battelle Memorial Institute, Engineering Property Data on Selected Ceramics, Vol. II. Carbides, MCIC-HB-07-Vol.II, Metals and Ceramics Information Center, Columbus, OH., 1979.

19. System Planning Corporation, Material Fabrication by SHS in the Soviet Union, Vol. II, SPC Report 81-4082, Defense Advanced Research Projects Agency (DARPA), Arlington, VA., 1982.

20. Schick, H. L., Thermodynamics of Certain Refractory Compounds., Volume 1, Academic Press, New York, NY., 1966.

21. Kieffer, R., "Preparation and Properties of Interstitial Compounds," J. Inst. Met., Vol. 97, No. 6, pp. 164-172, June 1969.

22. Brukl, C. E. and Harmon, D. P., Ternary Phase Equilibria in Transition Metal-Boron-Carbon-Silicon Systems, AFML-TR-65-2, Part II, Volume IV, Air Force Materials Laboratory, Wright-Patterson Air Force Base, OH., 1966.

Distribution List

| No of Copies | Organization |
|---|---|
| 12 | Administrator<br>Defense Technical Info Center<br>ATTN: DTIC-DDA<br>Cameron Station<br>Alexandria, VA 22304-6145 |
| 1 | HQDA (SARD-TR)<br>Washington, DC 20310-0001 |
| 1 | Commander<br>US Army Materiel Command<br>ATTN: AMCDRA-ST<br>5001 Eisenhower Avenue<br>Alexandria, VA 22333-0001 |
| 1 | Commander<br>US Army Laboratory Command<br>ATTN: AMSLC-DL<br>Adelphi, MD 20783-1145 |
| 2 | Commander<br>Armament RD&E Center<br>US Army AMCCOM<br>ATTN: SMCAR-MSI<br>Picatinny Arsenal, NJ 07806-5000 |
| 2 | Commander<br>Armament RD&E Center<br>US Army AMCCOM<br>ATTN: SMCAR-TDC<br>Picatinny Arsenal, NJ 07806-5000 |
| 1 | Director<br>Benet Weapons Laboratory<br>Armament RD&E Center<br>US Army AMCCOM<br>ATTN: SMCAR-LCB-TL<br>Watervliet, NY 12189-4050 |
| 1 | Commander<br>US Army Armament, Munitions<br>and Chemical Command<br>ATTN: SMCAR-ESP-L<br>Rock Island, IL 61299-5000 |
| 1 | Commander<br>US Army Aviation Systems Command<br>ATTN: AMSAV-DACL<br>4300 Goodfellow Blvd.<br>St. Louis, MO 63120-1798 |
| 1 | Director<br>US Army Aviation Research<br>and Technology Activity<br>Ames Research Center<br>Moffett Field, CA 94035-1099 |

| No. of Copies | Organization |
|---|---|
| 1 | Commander<br>US Army Missile Command<br>ATTN: AMSMI-AS<br>Redstone Arsenal, AL 35898-5010 |
| 1 | Commander<br>US Army Tank Automotive Command<br>ATTN: AMSTA-TSL (Technical Library)<br>Warren, MI 48397-5000 |
| 1 | Director<br>US Army TRADOC Analysis Command<br>ATTN: ATAA-SL<br>White Sands Missile Range, NM 88002-5502 |
| 1 | Commandant<br>US Army Infantry School<br>ATTN: ATSH-CD-CSO-OR<br>Fort Benning, GA 31905-5660 |
| 1 | AFWL/SUL<br>Kirtland AFB, NM 87117-5800 |
| 1 | Air Force Armament Laboratory<br>ATTN: AFATL/DLODL<br>Eglin AFB, FL 32542-5000 |
| 1 | Commander<br>ERADCOM Technical Library<br>ATTN: DELSD-L (Reports Section)<br>Fort Monmouth, NJ 07703-5301 |
| 1 | Commander<br>US Army Development<br>and Employment Agency<br>ATTN: MODE-TED-SAB<br>Fort Lewis, WA 98433 |
| 10 | Central Intelligence Agency<br>Office of Central Reference<br>Dissemination Branch<br>Room GE-47 HQS<br>Washington, DC 20502 |
| | Aberdeen Proving Ground<br>Dir, USAMSAA<br>ATTN: AMXSY-D<br>AMXSY-MP, H. Cohen<br>Cdr, USATECOM<br>ATTN: AMSTE-TO-F<br>Cdr, CRDEC, AMCCOM<br>ATTN: SMCCR-RSP-A<br>SMCCR-MU<br>SMCCR-SPS-IL<br>APG, MD 21005 |

USER EVALUATION SHEET/CHANGE OF ADDRESS

This laboratory undertakes a continuing effort to improve the quality of the reports it publishes. Your comments/answers below will aid us in our efforts.

1. Does this report satisfy a need? (Comment on purpose, related project, or other area of interest for which the report will be used.) _____

2. How, specifically, is the report being used? (Information source, design data, procedure, source of ideas, etc.) _____

3. Has the information in this report led to any quantitative savings as far as man-hours or dollars saved, operating costs avoided, or efficiencies achieved, etc? If so, please elaborate. _____

4. General Comments. What do you think should be changed to improve future reports? (Indicate changes to organization, technical content, format, etc.) _____

BRL Report Number _____ Division Symbol _____

Check here if desire to be removed from distribution list. ____

Check here for address change. ____

Current address: Organization _____
Address _____

----------FOLD AND TAPE CLOSED----------

Director
U.S. Army Ballistic Research Laboratory
ATTN: SLCBR-DD-T(NEI)
Aberdeen Proving Ground, MD 21005-5066

OFFICIAL BUSINESS
PENALTY FOR PRIVATE USE $300

**BUSINESS REPLY LABEL**
FIRST CLASS PERMIT NO. 12062 WASHINGTON D. C.
POSTAGE WILL BE PAID BY DEPARTMENT OF THE ARMY

NO POSTAGE NECESSARY IF MAILED IN THE UNITED STATES

Director
U.S. Army Ballistic Research Laboratory
ATTN: SLCBR-DD-T(NEI)
Aberdeen Proving Ground, MD 21005-9989